# Pilot-Based Channel Estimation for AF Relaying Using Energy Harvesting

Yunfei Chen, *Senior Member, IEEE*, Wei Feng, Rui Shi, Ning Ge

***Abstract*— In existing channel estimators for amplify-and-forward relaying, pilots are often sent from the relay to the destination which consumes the relay's own energy. This limits the relay's participation in the network. In this paper, several moment-based channel estimators for amplify-and-forward relaying are proposed that harvest energy from the source and using the harvested energy to send pilots to the destination for channel estimation. Both time-switching and power-splitting strategies are considered. Numerical results show that the two schemes that perform channel estimation only at the destination have worse performances than the two schemes that perform channel estimation at both the relay and the destination. They also show that the bit error rate performances of all schemes are close to the perfect case when exact knowledge of the channel state information is available such that there is no channel estimation error in the demodulation. The assumption that the two schemes only perform channel estimation at the destination makes them simpler, as they do not require channel estimation at the relay or feed the channel estimate back to the destination.**

***Index Terms*— Amplify-and-forward, channel estimation, energy harvesting, moments.**

## I. Introduction

In amplify-and-forward (AF) relaying, the amplification and forwarding operations at the relay consume energy. This may not be desirable for relays operating on batteries with limited lifetime, and may discourage them from taking part in relaying. To solve this problem, energy harvesting information relaying has been proposed [1] - [3], where the relay harvests energy from the source and uses only this energy to forward the information signal.

Energy harvesting (EH) is one of the recent advances in electronics. In particular, radio frequency (RF) energy harvesting can provide wireless power [4]. Among different RFEH techniques, far-field harvesting allows long-range energy transfer and therefore is suitable for communications systems. However, due to the long range, the harvested energy is often of milli-Watt or micro-Watt scale [5]. This restricts application to low-power systems, such as sensor networks [6]. Consequently, in [7], the use of electromagnetic waves for both information and energy transfer was studied. Two practical schemes, time-switching (TS) and power-splitting (PS), were studied in [8].

Yunfei Chen is with the School of Engineering, University of Warwick, Coventry, U.K. CV4 7AL (e-mail: Yunfei.Chen@warwick.ac.uk).

Rui Shi is with the School of Aerospace Engineering, Tsinghua University, Beijing 100084, China. e-mail: r.shi@mail.tsinghuamail.edu.cn.

Wei Feng and Ning Ge are with the Department of Electronic Engineering, Tsinghua University, Beijing 100084, P. R. China. e-mail: fengwei@tsinghua.edu.cn, gening@tsinghua.edu.cn

Channel estimation is an essential part of wireless relaying, as the destination needs the channel coefficients for demodulation, and the relay sometimes needs them for amplification. Several works have been conducted on channel estimation for relaying, which mainly focused on the minimum mean squared error (MMSE) estimation and the cascaded channel estimation, such as in [9], [10] and [12]. In [11], a least squares estimator was also proposed. In [13], the estimators for individual channel coefficients were used. In [14], the individual channel powers were estimated using moment-based (MB) estimators. All the aforementioned estimators were designed for conventional AF relaying, where the pilots used by the estimators in [9] - [14] have to be sent from the relay to the destination using the relay's own energy. It would be advantageous for the relay if the pilots could be sent without using the relay's own energy, that is, energy harvesting channel estimation. In this case, new and greater challenges occur. Due to energy harvesting, the cascaded channel coefficient is not a simple product of the channel coefficients in the source-to-relay and relay-to-destination links any more. Also, the individual channel gains will be always coupled with each other.

In this paper, new pilot-based channel estimators for AF relaying are proposed. The pilots are sent from the relay to the destination using energy harvested from the source. Channel estimation is performed only using these pilots multiplexed in the time domain with the data symbols for single-carrier systems. Both TS and PS strategies are considered. In TS, the source sends a group of pilots dedicated for energy harvesting in the first part of the frame and another group dedicated for channel estimation in the second part of the frame, while in PS, the source only sends one group of pilots with each pilot split in power for both energy harvesting and channel estimation. Fig. 1 describes and compares TS and PS. In Scheme 1 and Scheme 2, the relay harvests energy from the source and then uses this energy to forward both pilots from the source and its own pilots to the destination. In Scheme 3 and Scheme 4, the relay harvests energy from the source and also uses these to estimate the source-to-relay link. Then, the harvested energy is used to transmit its own pilot to the destination for the estimation of the relay-to-destination link. Numerical results are presented to show the good performances of these proposed estimators. The difference between this work and the previous works in [9] - [14] is that harvested energy is used for channel estimation in this work while the previous works use conventional battery energy. There are many works on energy harvesting data transmission, such as [1] - [3]. However, these use the harvested energy for information decoding but did not

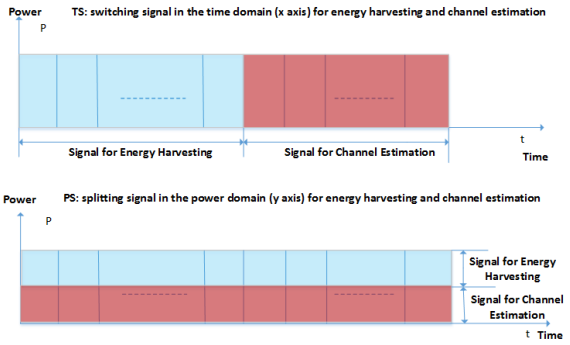


Fig. 1. Comparison of TS and PS strategies using the same total number of pilots.

consider channel estimation.

This paper has two main technical contributions: First, it is the first work to consider the use of energy harvesting for channel estimation in relaying, an important part of relaying. Previous works either considered the use of energy harvesting in data relaying without designing any channel estimators or designed channel estimators for data relaying without any energy harvesting. Our work makes new contribution by considering the use of energy harvesting for channel estimation in relaying. Second, our work provides four estimators with different performances and complexities, suitable for different applications. Detailed derivations of these estimators are presented, and analytical expressions of their performances are obtained. These results provide useful insights and important guidance on how to choose the system parameters for best performances. Thus, they make considerable contribution to relaying system designs.

The remainder of the paper is organized as follows. Section II derives the new estimators. In Section III, the first- and second-order moments of the estimators will be analyzed. Section IV will present numerical examples. Finally, concluding remarks will be made in Section V.

## II. New Estimators

Consider a wireless relaying network with one source, one relay and one destination. The signal is transmitted from the source to the destination via the relay. The following assumptions are used in the paper.

### A. Assumptions

- There is no direct link between the source and the destination. This is the case when the destination is out range of the source [15]. This is also the case when an obstacle exists between the source and the destination [16].
- All the nodes operate in half-duplex mode and have a single antenna for simplicity. Multiple antennas would incur more unknown channel coefficients and longer pilot sequences and are thus more complicated. This can be a future topic.
- All the schemes use time division protocol, where the first part of the time duration is for source-to-relay transmission and the second part of the time duration is for relay-to-destination transmission.
- A total of $K$ pilots are used in each scheme for energy harvesting and channel estimation.
- Each pilot occupies a time duration of $T_p$.
- Block Rayleigh fading is used such that all channel coefficients are complex Gaussian from block to block, but remain constant during channel estimation in one block.
- The pilot symbol has a value of 1 without loss of generality.
- All noise are circularly symmetric and complex additive white Gaussian noise (AWGN).
- For harvesting, the noise energy is small compared with the harvested signal energy and thus, assumed negligible (see the derivations of (5) - (13) in [8]).
- Fixed-gain relaying is used so that the amplification factor is a constant that normalizes the average power of the signal received at the relay [17], [18].

### B. Scheme 1

In Scheme 1, the relay harvests energy from the source using TS and then uses the harvested energy to forward pilots from the source as well as transmit its own pilots to the destination. Firstly, the source sends $I$ pilots to the relay for energy harvesting. The received signal at the relay is given by

$$y_{r-eh}^{(i)} = \sqrt{P_s} h s + n_{r-eh}^{(i)} \tag{1}$$

where $i = 1, 2, \cdots, I$, $P_s$ is the source transmission power, $h$ is the channel coefficient of the source-to-relay link and $h$ is a complex Gaussian random variable with zero mean and variance $2\alpha^2$, $s = 1$ is the pilot value and is omitted in the following, and $n_{r-eh}$ is the AWGN with zero mean and variance $2\sigma_r^2$. Using (1), the harvested energy is

$$E_h = \eta P_s |h|^2 I T_p \tag{2}$$

where $\eta$ is the conversion efficiency of the energy harvester and $IT_p$ is the total harvesting time. Note that $P_s|h|^2$ is the amount of radiated power from the source picked up by the harvester at its input. Due to path loss and fading, this amount is often small. For example, reference [19] reported that the input can be -8 dBm when the source radiates 4 Watts at a distance of 15 meters, and reference [20] reported that the input can be -11 dBm when the source radiates 0.32 Watts at a distance of 1.1 meters.

Secondly, the source sends another $J_1$ pilots to the relay, which will be forwarded to the destination for channel estimation. The received signal at the destination is

$$y_{d-s}^{(j_1)} = \sqrt{P_r} g a y_{r-ce}^{(j_1)} + n_{d-s}^{(j_1)}, \tag{3}$$

where $y_{r-ce}^{(j_1)} = \sqrt{P_s} h + n_{r-ce}^{(j_1)}$ is the forwarded signal, $j_1 = 1, 2, \cdots, J_1$, $n_{r-ce}^{(j_1)}$ is the AWGN at the relay with mean zero and variance $2\sigma_r^2$, $P_r$ is the relay transmission power, $g$ is the channel coefficient of the relay-to-destination link and $g$ is a complex Gaussian random variable with zero mean and variance $2\alpha^2$, $a$ is the amplification factor, and $n_{d-s}^{(j_1)}$ is the AWGN at the destination with zero mean and variance $2\sigma_d^2$.

Finally, in addition to forwarding $J_1$ pilots from the source, the relay also uses the harvested energy to transmit $J_2$ pilots of its own to the destination, giving

$$y_{d-r}^{(j_2)} = \sqrt{P_r} g + n_{d-r}^{(j_2)} \tag{4}$$

where $j_2 = 1, 2, \cdots, J_2$, $n_{d-r}^{(j_2)}$ is the AWGN at the destination during this transmission and is again complex Gaussian with zero mean and variance $2\sigma_d^2$. Note that the relay transmits $J_2$ pilots of its own to the destination after it forwards the $J_1$ pilots from the source. Thus, they are orthogonal in time and will not interfere. Using the harvested energy in (2), since the relay has to forward $J_1$ pilots from the source and transmit $J_2$ pilots of its own, the transmission power of the relay in (3) and (4) can be written as

$$P_r = \frac{E_h}{JT_p} = \eta P_s |h|^2 \frac{I}{J} \tag{5}$$

where $J = J_1 + J_2$. Note that (5) is obtained by dividing the total harvested energy by the total transmission time. The amplification factor $a$ is used to normalize the average power of the forwarded signal $y_{r-ce}^{(j_1)}$ [17], [18]. Thus, $a^2 E\{|y_{r-ce}^{(j_1)}|^2\}$ often gives one and they do not appear in $J$. Next, we derive the new estimators for $g$ and $h$. From (4), one has

$$y_{d-r}^{(j_2)} = \sqrt{\eta \frac{I}{J} P_s} |h| g + n_{d-r}^{(j_2)} \tag{6}$$

and from (3), one has

$$y_{d-s}^{(j_1)} = \sqrt{\eta \frac{I}{J}} P_s |h| g h a + \sqrt{\eta \frac{I}{J} P_s} |h| g a n_{r-ce}^{(j_1)} + n_{d-s}^{(j_1)}. \tag{7}$$

It is well-known that the MB estimators are often simpler than other estimators. In some cases, they also provide efficient estimation [21]. Thus, they are considered first. The first-order moments of (6) and (7) are

$$E\{y_{d-r}^{(j_2)}\} = \sqrt{\eta \frac{I}{J} P_s} |h| g \tag{8}$$

$$E\{y_{d-s}^{(j_1)}\} = \sqrt{\eta \frac{I}{J}} P_s |h| g h a. \tag{9}$$

One can approximate $E\{y_{d-r}^{(j_2)}\}$ using $\frac{1}{J_2}\sum_{j_2=1}^{J_2} y_{d-r}^{(j_2)}$, and $E\{y_{d-s}^{(j_1)}\}$ using $\frac{1}{J_1}\sum_{j_1=1}^{J_1} y_{d-s}^{(j_1)}$. Solving the equations in (8) and (9) for $g$ and $h$, one has the MB estimators for $g$ and $h$ in Scheme 1 as

$$\hat{g}_1 = \frac{\frac{1}{J_2}\sum_{j_2=1}^{J_2} y_{d-r}^{(j_2)} | \frac{1}{J_2}\sum_{j_2=1}^{J_2} y_{d-r}^{(j_2)}|}{\frac{1}{a}\sqrt{\eta \frac{I}{J}} | \frac{1}{J_1}\sum_{j_1=1}^{J_1} y_{d-s}^{(j_1)}|} \tag{10}$$

$$\hat{h}_1 = \frac{1}{\sqrt{P_s} a} \frac{\frac{1}{J_1}\sum_{j_1=1}^{J_1} y_{d-s}^{(j_1)}}{\frac{1}{J_2}\sum_{j_2=1}^{J_2} y_{d-r}^{(j_2)}} \tag{11}$$

respectively. Note that other orders of moments can also be used but the lower the order is, the better the MB estimator will be in terms of variance [21]. Thus, we use the first order. Other alternatives include the maximum likelihood (ML) method, the least squares (LS) method and the MMSE method. The ML estimator can be derived by maximizing the log-likelihood function, which can be shown as a highly nonlinear function of $g$ and $h$. Thus, it does not lead to estimators as simple as the MB estimators. For Gaussian noise, the LS method normally gives the same estimator as the ML method. Also, the MMSE is for time-selective channels, while we assume time-non-selective channels here, and Thus, it is not applicable. Since both $y_{d-s}^{(j_1)}$ and $y_{d-r}^{(j_2)}$ are received at the destination, the relay does not perform channel estimation. This reduces the complexity at the relay.

### C. Scheme 2

Scheme 2 is similar to Scheme 1, except that the energy is harvested using the PS strategy. Firstly, the source sends $K_1$ pilots to the relay. Part of the received signal at the relay is used for channel estimation, where $z_{r-ce}^{(k_1)} = \sqrt{(1-\rho)P_s} h + n_{r-ce}^{(k_1)}$ is forwarded to the destination as

$$z_{d-s}^{(k_1)} = \sqrt{P_r} g a z_{r-ce}^{(k_1)} + n_{d-s}^{(k_1)} \tag{12}$$

where $k_1 = 1, 2, \cdots, K_1$ index the pilots from the source, $\rho$ is the PS factor, $n_{r-ce}^{(k_1)}$ and $n_{d-s}^{(k_1)}$ are the AWGN with zero means and variances $2\sigma_r^2$ and $2\sigma_d^2$, respectively. The other part of the received power at the relay is harvested as $E_h = \eta\rho P_s |h|^2 K_1 T_p$.

Secondly, the relay also transmits $K_2$ of its own pilots to the destination such that the received signal at the destination is

$$z_{d-r}^{(k_2)} = \sqrt{P_r} g + n_{d-r}^{(k_2)} \tag{13}$$

where $k_2 = 1, 2, \cdots, K_2$ and $n_{d-r}^{(k_2)}$ is the AWGN with zero mean and variance $2\sigma_d^2$.

Since the relay forwards $K_1$ pilots from the source and transmits $K_2$ pilots of its own, a total of $K = K_1 + K_2$ pilots will be sent to the destination such that

$$P_r = \frac{E_h}{KT_p} = \eta\rho P_s |h|^2 \frac{K_1}{K}. \tag{14}$$

Again, since $a$ normalizes the average power of $z_{r-ce}^{(k_1)}$, it does not appear in $K$. Thus, one can substitute (14) in (13) to obtain

$$z_{d-r}^{(k_2)} = \sqrt{\eta\rho P_s \frac{K_1}{K}} |h| g + n_{d-r}^{(k_2)} \tag{15}$$

and one can substitute (14) in (12) as

$$z_{d-s}^{(k_1)} = \sqrt{\eta\rho(1-\rho)\frac{K_1}{K}} P_s |h| g h a + \sqrt{\eta\rho P_s \frac{K_1}{K}} |h| g a n_{r-ce}^{(k_1)} + n_{d-s}^{(k_1)}. \tag{16}$$

The first-order moments of $z_{d-r}^{(k_2)}$ and $z_{d-s}^{(k_1)}$ are

$$E\{z_{d-r}^{(k_2)}\} = \sqrt{\eta\rho P_s \frac{K_1}{K}} |h| g \tag{17}$$

$$E\{z_{d-s}^{(k_1)}\} = \sqrt{\eta\rho(1-\rho)\frac{K_1}{K}} P_s |h| g h a. \tag{18}$$

Thus, the MB estimators for $g$ and $h$ can be derived from (17) and (18) as

$$\hat{g}_2 = \frac{a\sqrt{1-\rho}}{\sqrt{\eta\rho\frac{K_1}{K}}} \frac{\frac{1}{K_2}\sum_{k_2=1}^{K_2} z_{d-r}^{(k_2)} | \frac{1}{K_2}\sum_{k_2=1}^{K_2} z_{d-r}^{(k_2)}|}{|\frac{1}{K_1}\sum_{k_1=1}^{K_1} z_{d-s}^{(k_1)}|} \tag{19}$$

and

$$\hat{h}_2 = \frac{1}{\sqrt{(1-\rho)P_s}a}\frac{\frac{1}{K_1}\sum_{k_1=1}^{K_1} z_{d-s}^{(k_1)}}{\frac{1}{K_2}\sum_{k_2=1}^{K_2} z_{d-r}^{(k_2)}} \tag{20}$$

respectively. Again, the ML estimators are too complicated and not derived here. Also, only the destination needs to perform channel estimation and thus reduces complexity at the relay.

### D. Scheme 3

In Scheme 3, firstly, the source sends $J_1$ pilots to the relay such that the received signal at the relay is

$$u_{r-ce}^{(j_1)} = \sqrt{P_s}h + n_{r-ce}^{(j_1)} \tag{21}$$

where $j_1 = 1, 2, \cdots, J_1$ and $n_{r-ce}^{(j_1)}$ is the AWGN with zero mean and variance $2\sigma_r^2$. Secondly, the source sends $I$ pilots to the relay for energy harvesting. The harvested energy $E_h = \eta P_s|h|^2 I T_p$. Finally, the relay uses the harvested energy to transmit $J_2$ pilots of its own to the destination. The transmission power of the relay is $P_r = \frac{E_h}{J_2 T_p} = \eta P_s|h|^2\frac{I}{J_2}$ and the received signal at the destination is

$$u_{d-r}^{(j_2)} = \sqrt{\eta P_s \frac{I}{J_2}}|h|g + n_{d-r}^{(j_2)} \tag{22}$$

where $j_2 = 1, 2, \cdots, J_2$. Again, the relay transmits $J_2$ pilots of its own to the destination after it forwards the $J_1$ pilots from the source. Thus, they are orthogonal in time and will not interfere. From (21) and (22), one has

$$E\{u_{r-ce}^{(j_1)}\} = \sqrt{P_s}h \tag{23}$$

$$E\{u_{d-r}^{(j_2)}\} = \sqrt{\eta P_s \frac{I}{J_2}}|h|g. \tag{24}$$

Thus, the MB estimators are derived by solving (23) and (24) as

$$\hat{g}_3 = \frac{\frac{1}{J_2}\sum_{j_2=1}^{J_2} u_{d-r}^{(j_2)}}{\sqrt{\eta\frac{I}{J_2}}|\frac{1}{J_1}\sum_{j_1=1}^{J_1} u_{r-ce}^{(j_1)}|} \tag{25}$$

and

$$\hat{h}_3 = \frac{1}{\sqrt{P_s}}\frac{1}{J_1}\sum_{j_1=1}^{J_1} u_{r-ce}^{(j_1)}. \tag{26}$$

Note that, in this scheme, the relay estimates $h$ and its estimate has to be fed back to the destination via control channels for the estimation of $g$ at the destination. Thus, this scheme is more complicated than Scheme 1 and Scheme 2.

### E. Scheme 4

Scheme 4 is similar to Scheme 3, except the relay uses PS to harvest energy. Firstly, the source sends $K_1$ pilots to the relay, part of which is received for channel estimation as

$$v_{r-ce}^{(k_1)} = \sqrt{(1-\rho)P_s}h + n_{r-ce}^{(k_1)} \tag{27}$$

for $k_1 = 1, 2, \cdots, K_1$ and part of which is harvested with $E_h = \eta\rho P_s|h|^2 K_1 T_p$. Secondly, the relay uses the harvested energy to transmit $K_2$ pilots of its own such that the received signal at the destination is

$$v_{d-r}^{(k_2)} = \sqrt{\eta\rho P_s \frac{K_1}{K_2}}|h|g + n_{d-r}^{(k_2)} \tag{28}$$

for $k_2 = 1, 2, \cdots, K_2$.

Similarly, using (27) and (28), the MB estimators for $g$ and $h$ can be derived as

$$\hat{g}_4 = \frac{\frac{1}{K_2}\sum_{k_2=1}^{K_2} v_{d-r}^{(k_2)}}{\sqrt{\eta\frac{K_1}{K_2}\frac{\rho}{1-\rho}}|\frac{1}{K_1}\sum_{k_1=1}^{K_1} v_{r-ce}^{(k_1)}|} \tag{29}$$

and

$$\hat{h}_4 = \frac{1}{\sqrt{(1-\rho)P_s}}\frac{1}{K_1}\sum_{k_1=1}^{K_1} v_{r-ce}^{(k_1)}. \tag{30}$$

## III. Estimator Performance

In this section, we derive the first- and second-order moments of the estimates to examine the performances of the new estimators.

### A. Scheme 1

For Scheme 1, denote $y_r = \frac{1}{J_2}\sum_{j_2=1}^{J_2} y_{d-r}^{(j_2)} = r_{y_r}e^{j\theta_{y_r}}$ and $y_s = \frac{1}{J_1}\sum_{j_1=1}^{J_1} y_{d-s}^{(j_1)} = r_{y_s}e^{j\theta_{y_s}}$. One sees that $y_r$ and $y_s$ are complex Gaussian random variables with means $S_{y_r} = \sqrt{\eta\frac{I}{J}P_s}|h|g$ and $S_{y_s} = \sqrt{\eta\frac{I}{J}P_s}|h|gha$, and variances $2\beta_{y_r}^2 = \frac{2\sigma_d^2}{J_2}$ and $2\beta_{y_s}^2 = \frac{2}{J_1}(\sigma_d^2 + \eta\frac{I}{J}P_s|h|^2|g|^2a^2\sigma_r^2)$, respectively. Thus, $r_{y_r}$ and $r_{y_s}$ are Rician random variables.

From (10), one has

$$E\{\hat{g}_1\} = \frac{a}{\sqrt{\eta\frac{I}{J}}}E\{r_{y_r}^2 e^{j\theta_{y_r}}\}E\{\frac{1}{r_{y_s}}\} \tag{31}$$

where $E\{r_{y_r}^2 e^{j\theta_{y_r}}\} = \frac{3\beta_{y_r}^2 e^{-\frac{|S_{y_r}|^2}{2\beta_{y_r}^2}}}{\pi}\int_0^{2\pi} e^{j\theta_{y_r} + \frac{|S_{y_r}|^2\cos^2(\theta_{y_r}+\epsilon)}{4\beta_{y_r}^2}} D_{-4}(-\frac{|S_{y_r}|\cos(\theta_{y_r}+\epsilon)}{\beta_{y_r}})d\theta_{y_r}$, using [22, eq. (3.462.1)] and [23, eq. (A.29)], and $E\{\frac{1}{r_{y_s}}\} = \frac{\sqrt{\pi}e^{-\frac{|S_{y_s}|^2}{4\beta_{y_s}^2}}}{\sqrt{2\beta_{y_s}^2}}I_0(\frac{|S_{y_s}|^2}{4\beta_{y_s}^2})$, using [22, eq. (6.618.4)] and [23, eq. (2.45)], $\epsilon$ is the negative of the phase angle of $g$, $D_{-4}(\cdot)$ is the parabolic cylinder function [22, eq. (9.240)] and $I_0(\cdot)$ is the zero-th order modified Bessel function of the first kind [22, eq. (8.406.1)]. One sees that, when $\sigma_d^2$ is negligible, $\frac{|S_{y_s}|^2}{\beta_{y_s}^2} \approx \frac{J_1 P_s|h|^2}{2\sigma_r^2}$. Thus, when $J_1$ or the signal-to-noise ratio (SNR) in the source-to-relay link $\frac{P_s|h|^2}{2\sigma_r^2}$ increases, $E\{\frac{1}{r_{y_s}}\}$ decreases rapidly due to the exponential and Bessel functions. This reduces the mean of $\hat{g}_1$ in (31).

Also, from (11), one has

$$E\{\hat{h}_1\} = \frac{S_{y_s}}{\sqrt{P_s}a}E\{\frac{1}{r_{y_r}}e^{-j\theta_{y_r}}\} \tag{32}$$

where $E\{\frac{1}{r_{y_r}}e^{-j\theta_{y_r}}\} = \frac{1}{\sqrt{2\pi\beta_{y_r}^2}}\int_0^{2\pi} e^{-j\theta_{y_r} - \frac{|S_{y_r}|^2\sin^2(\theta_{y_r}+\epsilon)}{2\beta_{y_r}^2}} Q(-|S_{y_r}|\cos(\theta_{y_r}+\epsilon)/\beta_{y_r})d\theta_{y_r}$ and $Q(\cdot)$ is the Gaussian Q function. One has $\frac{|S_{y_r}|^2}{\beta_{y_r}^2} = \frac{\eta\frac{J_2 I}{J}P_s|h|^2|g|^2}{2\sigma_d^2}$ and $\frac{S_{y_s}}{\sqrt{P_s}a} =$

$\sqrt{\eta\frac{I}{J}P_s}|h|gh$. Thus, from (32), when $J_2$ increases or $\sigma_d^2$ decreases, $E\{\frac{1}{r_{y_r}}e^{-j\theta_{y_r}}\}$ decreases such that the mean of $\hat{h_1}$ reduces. The mean of $\hat{h}_1$ does not depend on $a$. Both $\hat{g_1}$ and $\hat{h}_1$ are biased estimators. The second-order moments can be derived as follows.

From (10), one has

$$E\{|\hat{g}_1|^2\} = \frac{a^2}{\eta\frac{I}{J}}E\{r_{y_r}^4\}E\{\frac{1}{r_{y_s}^2}\} \tag{33}$$

where $E\{r_{y_r}^4\} = 2(2\beta_{y_r}^2)^2 + 4(2\beta_{y_r}^2)|S_{y_r}|^2 + |S_{y_r}|^4$ using moments of a Rician random variable and $E\{\frac{1}{r_{y_s}^2}\} = \int_0^\infty \frac{1}{\beta_{y_s}^2 x}e^{-\frac{x^2+|S_{y_s}|^2}{2\beta_{y_s}^2}}I_0(\frac{x|S_{y_s}|}{\beta_{y_s}^2})dx$, using [23, eq. (2.45)]. Also, from (11), one has

$$E\{|\hat{h}_1|^2\} = \frac{1}{P_s a^2}E\{r_{y_s}^2\}E\{\frac{1}{r_{y_r}^2}\} \tag{34}$$

where $E\{r_{y_s}^2\} = 2\beta_{y_s}^2 + |S_{y_s}|^2$ and $E\{\frac{1}{r_{y_r}^2}\} = \int_0^\infty \frac{1}{\beta_{y_r}^2 x}e^{-\frac{x^2+|S_{y_r}|^2}{2\beta_{y_r}^2}}I_0(\frac{x|S_{y_r}|}{\beta_{y_r}^2})dx$. One can see from (33) and (34) that the second-order moment of $\hat{g}_1$ decreases with $J_2$, while the second-order moment of $\hat{h}_1$ decreases with $J_1$ and $a^2$, respectively.

### B. Scheme 2

In this subsection, we derive the first- and second-order moments of $\hat{g}_2$ and $\hat{h}_2$. Denote $z_r = \frac{1}{K_2}\sum_{k_2=1}^{K_2} z_{d-r}^{(k_2)} = r_{z_r}e^{j\theta_{z_r}}$ and $z_s = \frac{1}{K_1}\sum_{k_1=1}^{K_1} z_{d-s}^{(k_1)} = r_{z_s}e^{j\theta_{z_s}}$, which are complex Gaussian with means $S_{z_r} = \sqrt{\eta\rho P_s\frac{K_1}{K}}|h|g$ and $S_{z_s} = \sqrt{\eta\rho(1-\rho)\frac{K_1}{K}P_s}|h|ghha$, and variances $2\beta_{z_r}^2 = \frac{2\sigma_d^2}{K_2}$ and $2\beta_{z_s}^2 = \frac{2}{K_1}(\sigma_d^2 + \eta\rho P_s|h|^2|g|^2a^2\sigma_r^2\frac{K_1}{K})$, respectively.

From (19) and (20), the first-order moments can be derived as

$$E\{\hat{g}_2\} = \frac{a}{\sqrt{\eta\frac{K_1}{K}}}\sqrt{\frac{1-\rho}{\rho}}E\{r_{z_r}^2e^{j\theta_{z_r}}\}E\{\frac{1}{r_{z_s}}\} \tag{35}$$

$$E\{\hat{h}_2\} = \sqrt{\eta\rho P_s\frac{K_1}{K}}|h|ghE\{\frac{1}{r_{z_r}}e^{-j\theta_{z_r}}\} \tag{36}$$

where $E\{\frac{1}{r_{z_r}}e^{-j\theta_{z_r}}\}$, $E\{r_{z_r}^2e^{j\theta_{z_r}}\}$ and $E\{\frac{1}{r_{z_s}}\}$ are obtained by replacing $S_{y_r}$, $\beta_{y_r}$, $S_{y_s}$ and $\beta_{y_s}$ with $S_{z_r}$, $\beta_{z_r}$, $S_{z_s}$ and $\beta_{z_s}$ in $E\{\frac{1}{r_{y_r}}e^{-j\theta_{y_r}}\}$, $E\{r_{y_r}^2e^{j\theta_{y_r}}\}$ and $E\{\frac{1}{r_{y_s}}\}$, respectively. Similar insights can be obtained. Again, both $\hat{g_2}$ and $\hat{h_2}$ are biased estimators. The mean of $\hat{g_2}$ decreases when $K_1$ or the SNR of the source-to-relay link increase, and the mean of $\hat{h_2}$ decreases when $K_2$ increases or $\sigma_d^2$ decreases.

For the second-order moments, one has

$$E\{|\hat{g}_2|^2\} = \frac{a^2}{\eta\frac{K_1}{K}}\frac{1-\rho}{\rho}E\{r_{z_r}^4\}E\{\frac{1}{r_{z_s}^2}\} \tag{37}$$

and

$$E\{|\hat{h}_2|^2\} = \frac{1}{(1-\rho)P_s a^2}E\{r_{z_s}^2\}E\{\frac{1}{r_{z_r}^2}\} \tag{38}$$

where $E\{r_{z_r}^4\}$, $E\{\frac{1}{r_{z_s}^2}\}$, $E\{r_{z_s}^2\}$ and $E\{\frac{1}{r_{z_r}^2}\}$ are derived by replacing $S_{y_r}$, $\beta_{y_r}$, $S_{y_s}$ and $\beta_{y_s}$ with $S_{z_r}$, $\beta_{z_r}$, $S_{z_s}$ and $\beta_{z_s}$ in $E\{r_{y_r}^4\}$, $E\{\frac{1}{r_{y_s}^2}\}$, $E\{r_{y_s}^2\}$ and $E\{\frac{1}{r_{y_r}^2}\}$, respectively. Thus, the second-order moment of $\hat{g}_2$ decreases when $a^2$ or $\sigma_d^2$ decrease or when $K_2$ increases, and the second-order moment of $\hat{h}_2$ decreases when $a^2$ increases for small $\sigma_d^2$.

### C. Scheme 3

In Scheme 3, we denote $u_r = \frac{1}{J_2}\sum_{j_2=1}^{J_2} u_{d-r}^{(j_2)} = r_{u_r}e^{j\theta_{u_r}}$ and $u_s = \frac{1}{J_1}\sum_{j_1=1}^{J_1} u_{r-ce}^{(j_1)} = r_{u_s}e^{j\theta_{u_s}}$. Then, $u_r$ and $u_s$ are complex Gaussian random variables with means $S_{u_r} = \sqrt{\eta P_s\frac{I}{J_2}}|h|g$ and $S_{u_s} = \sqrt{P_s}h$, and variances $2\beta_{u_r}^2 = \frac{2\sigma_d^2}{J_2}$ and $2\beta_{u_s}^2 = \frac{2\sigma_r^2}{J_1}$.

In this case, one has

$$E\{\hat{g}_3\} = \sqrt{P_s}|h|gE\{\frac{1}{r_{u_s}}\} \tag{39}$$

$$E\{\hat{h}_3\} = h \tag{40}$$

$$E\{|\hat{g}_3|^2\} = \frac{J_2}{\eta I}E\{r_{u_r}^2\}E\{\frac{1}{r_{u_s}^2}\} \tag{41}$$

$$E\{|\hat{h}_3|^2\} = \frac{2\sigma_r^2}{P_s J_1} + |h|^2. \tag{42}$$

where $E\{r_{u_r}^2\} = 2\beta_{u_r}^2 + |S_{u_r}|^2$, $E\{\frac{1}{r_{u_s}}\}$ and $E\{\frac{1}{r_{u_s}^2}\}$ can be obtained by replacing $S_{y_s}$ and $\beta_{y_s}$ with $S_{u_s}$ and $\beta_{u_s}$ in $E\{\frac{1}{r_{y_s}}\}$ and $E\{\frac{1}{r_{y_s}^2}\}$, respectively. One sees from (40) that $\hat{h}_3$ is an unbiased estimator. On the other hand, $\hat{g}_3$ is biased but becomes unbiased if the estimate is divided by $\sqrt{P_s}|h|E\{\frac{1}{r_{u_s}}\}$, which is a function of $h$ only. When $J_1$ or the SNR of the source-to-relay link increase, the mean of $\hat{g}_3$ decreases. Also, the second-order moment of $\hat{g}_3$ decreases when $\sigma_d^2$ decreases or when $\eta$ and $I$ increase, while the second-order moment of $\hat{h}_3$ decreases when $\sigma_r^2$ decreases or when $P_s$ and $J_1$ increase.

### D. Scheme 4

In Scheme 4, let $v_r = \frac{1}{K_2}\sum_{k_2=1}^{K_2} v_{d-r}^{(k_2)} = r_{v_r}e^{j\theta_{v_r}}$ and $v_s = \frac{1}{K_1}\sum_{k_1=1}^{K_1} v_{r-ce}^{(k_1)} = r_{v_s}e^{j\theta_{v_s}}$ so that $v_r$ is a complex Gaussian random variable with mean $S_{v_r} = \sqrt{\eta\rho P_s\frac{K_1}{K_2}}|h|g$ and variance $2\beta_{v_r}^2 = \frac{2\sigma_d^2}{K_2}$, and $v_s$ is a complex Gaussian random variable with mean $S_{v_s} = \sqrt{(1-\rho)P_s}h$ and variance $2\beta_{v_s}^2 = \frac{2\sigma_r^2}{K_1}$.

Then, following similar procedures, one has

$$E\{\hat{g}_4\} = \sqrt{(1-\rho)P_s}|h|gE\{\frac{1}{r_{v_s}}\}, \tag{43}$$

$$E\{\hat{h}_4\} = h, \tag{44}$$

$$E\{|\hat{g}_4|^2\} = \frac{2\sigma_d^2 + \eta K_1\rho P_s|h|^2|g|^2}{\eta K_1\rho/(1-\rho)}E\{\frac{1}{r_{v_s}^2}\}, \tag{45}$$

$$E\{|\hat{h}_4|^2\} = \frac{2\sigma_r^2}{(1-\rho)P_s K_1} + |h|^2, \tag{46}$$

where $E\{\frac{1}{r_{v_s}}\}$ and $E\{\frac{1}{r_{v_s}^2}\}$ are obtained by replacing $S_{y_s}$ and $\beta_{y_s}$ with $S_{v_s}$ and $\beta_{v_s}$ in $E\{\frac{1}{r_{y_s}}\}$ and $E\{\frac{1}{r_{y_s}^2}\}$, respectively.

Again, $\hat{h_4}$ is unbiased and $\hat{g_4}$ is biased. However, it can become unbiased by dividing the estimate by both $S_{v_s}$ and $E\{\frac{1}{r_{v_s}}\}$. Also, one sees that $\hat{g_4}$ does not depend on $\eta$. The TS and PS strategies can be compared using their variances. One can derive that $Var\{\hat{g}_3\} = \frac{2\sigma_d^2}{\eta I}E\{\frac{1}{r_{u_s}^2}\} + P_s|h|^2|g|^2(E\{\frac{1}{r_{u_s}^2}\} - E^2\{\frac{1}{r_{u_s}}\})$ and $Var\{\hat{h}_3\} = \frac{2\sigma_r^2}{P_s J_1}$ for TS, and $Var\{\hat{g}_4\} = \frac{2\sigma_d^2(1-\rho)}{\eta K_1 \rho}E\{\frac{1}{r_{v_s}^2}\} + (1-\rho)P_s|h|^2|g|^2(E\{\frac{1}{r_{v_s}^2}\} - E^2\{\frac{1}{r_{v_s}}\})$ and $Var\{\hat{h}_3\} = \frac{2\sigma_r^2}{(1-\rho)P_s K_1}$ for PS, where $E\{\frac{1}{r_{u_s}^2}\}$ is similar to $E\{\frac{1}{r_{v_s}^2}\}$ and $E\{\frac{1}{r_{u_s}}\}$ is similar to $E\{\frac{1}{r_{v_s}}\}$ except that $E\{\frac{1}{r_{u_s}^2}\}$ and $E\{\frac{1}{r_{u_s}}\}$ are determined by $\frac{|S_{u_s}|^2}{2\beta_{u_s}^2} = \frac{J_1 P_s|h|^2}{2\sigma_r^2}$ while $E\{\frac{1}{r_{v_s}^2}\}$ and $E\{\frac{1}{r_{v_s}}\}$ are determined by $\frac{|S_{v_s}|^2}{2\beta_{v_s}^2} = \frac{K_1(1-\rho)P_s|h|^2}{2\sigma_r^2}$. Thus, the performances of the TS and PS strategies depend on the choice of parameters. For example, if $J_1 > (1-\rho)K_1$, the variance of $\hat{h}_3$ for TS will be smaller than that of $\hat{h}_4$ for PS, but otherwise PS will outperform TS. Also, if $J_1 = K_1$ and $(1-\rho)P_s$ in PS is chosen to be the same as $P_s$ in TS, the variance of $\hat{g}_3$ for TS will be smaller than that of $\hat{g}_4$ for PS when $I > K_1\rho/(1-\rho)$ and vice versa.

The above analytical expressions can be used to calculate the MSE and the bias of the estimators, as the bias is determined by the first-order moment and the MSE is determined by the first-order and the second-order moments. The 1D integrals in these results can be easily and quickly calculated using standard mathematical software, such as MATLAB and Mathematica, in less than one second. In contrast, simulation of a smooth MSE curve often takes minutes or hours. Also, these analytical expressions give insights into the estimator performance. For example, the bias of $\hat{g}_1$ and the bias of $\hat{g}_2$ do not depend on the fading phase of $y_s$ and $z_s$, respectively, and $\hat{h}_1$ and $\hat{h}_2$ are asymptotically unbiased when the signal-to-noise ratio is large. Thus, these expressions are useful. All the above equations are newly derived, not from the literature. One can see that the derivation of the estimators in Section II and the performance analysis of the derived estimators in Section III are neither simple nor straightforward. They are novelty. The proposed estimators are simple but provide very high accuracy, as will be seen in the next section. The contribution of our work is to provide simple estimators with excellent performance.

## IV. Numerical Results and Discussion

In this section, the MSE and uncoded bit error rate (BER) performances of the newly derived estimators will be examined. In the examination, we fix $\eta = 0.5$, $P_s = 1$, $K = 100$ and $2\sigma_r^2 = 2\sigma_d^2 = 2$ to focus on the more important parameters. Define $\gamma_g = \frac{|g|^2}{2\sigma_d^2}$ as the instantaneous SNR of the relay-to-destination link, and $\gamma_h = \frac{|h|^2}{2\sigma_r^2}$ as the instantaneous SNR of the source-to-relay link. Their corresponding average SNRs are $\bar{\gamma}_g = \frac{E\{|g|^2\}}{2\sigma_d^2}$ and $\bar{\gamma}_h = \frac{E\{|h|^2\}}{2\sigma_r^2}$, respectively. The value of $a$ is set to normalize the power of the forwarded signal [17], [18]. For fixed channel realization, the values of $g$ and $h$ will be changed with $\gamma_g$ and $\gamma_h$ and their real and imaginary parts will be equal to each other. The normalized mean squared error (MSE) is defined as $\frac{1}{R|g|^2}\sum_{r=1}^{R}|\hat{g}_r - g|^2$, $\frac{1}{R|h|^2}\sum_{r=1}^{R}|\hat{h}_r - h|^2$, and $\frac{1}{R|gh|^2}\sum_{r=1}^{R}|\hat{g}_r\hat{h}_r - gh|^2$ for $\hat{g}$, $\hat{h}$ and $\hat{g}\hat{h}$, respectively, where $R$ is the total number of simulation runs and $\hat{g}_r$ and $\hat{h}_r$ are the channel estimates in the $r$-th run. For different channel realizations, the values of $E\{|g|^2\}$ and $E\{|h|^2\}$ will change with $\bar{\gamma}_g$ and $\bar{\gamma}_h$, assuming $\bar{\gamma}_g = \bar{\gamma}_h = \gamma_a$ as the average power for Rayleigh fading coefficients. The average normalized MSE is defined as $\frac{1}{QR|g_q|^2}\sum_{r=1}^{R}\sum_{q=1}^{Q}|\hat{g}_{r,q} - g_q|^2$, $\frac{1}{QR|h_q|^2}\sum_{r=1}^{R}\sum_{q=1}^{Q}|\hat{h}_{r,q} - h_q|^2$, and $\frac{1}{QR|g_q h_q|^2}\sum_{r=1}^{R}\sum_{q=1}^{Q}|\hat{g}_{r,q}\hat{h}_{r,q} - g_q h_q|^2$, where $Q$ is the number of channel realizations, and $\hat{g}_{r,q}$ and $\hat{h}_{r,q}$ are the channel estimates in the $r$-th run of the $q$-th channel realization. The average BER for different channel realizations will also be studied for binary phase shift keying (BPSK) as $BER = \frac{1}{QR}\sum_{r=1}^{R}\sum_{q=1}^{Q} I(Re\{y_{r,q}\hat{g}_{r,q}^*\hat{h}_{r,q}^*\} < 0)$, where $y_{r,q} = \sqrt{P_s}gha + gan_{r,q}^r + n_{r,q}^d$ is the received data signal at the destination, $I(\cdot)$ is the indicator function with $I(x) = 1$ when $x$ is true, and $n_{r,q}^r$ and $n_{r,q}^d$ are the AWGN at the relay and the destination, respectively, in the $r$-th run of the $q$-th channel realization. In the figures, the normalized MSE and BER in the y axis are in log scale, and the SNR in the x axis is in dB scale.

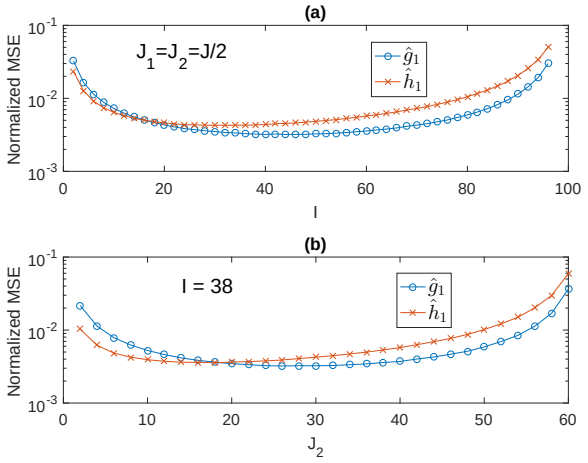


Fig. 2. Normalized MSE of $\hat{g}_1$ and $\hat{h}_1$ vs. $I$ and $J_2$ for $\gamma_g = \gamma_h = 10\ dB$ with fixed channel realization in Scheme 1.

Fig. 2 shows the normalized MSE of $\hat{g}_1$ and $\hat{h}_1$ in Scheme 1 versus the values of $I$ and $J_2$, when $\gamma_g = \gamma_h = 10\ dB$ with fixed channel realization. In Fig. 2.(a), we set $J_1 = J_2 = \frac{J}{2}$ to focus on $I$ from 4 to 96 with a step size of 4. In Fig. 2.(b), we set $I = 38$ to focus on $J_2$ from 2 to $J-2$ with a step size of 2. Two observations can be made. Firstly, from Fig. 2, the normalized MSE first decreases and then increases when the values of $I$ or $J_2$ increase, as expected, as a larger value of $I$ leads to more harvested energy such that the estimation at the destination node will be more accurate. It also leads to a smaller value of $J$ due to a fixed $K$ such that the sample size in the estimation reduces. Also, a larger value of $J_2$ leads to a better estimate of $\frac{1}{J_2}\sum_{j_2=1}^{J_2} y_{d-r}^{(j_2)}$ but due to fixed $J$ it also leads to a worse estimate of $\frac{1}{J_1}\sum_{j_1=1}^{J_1} y_{d-s}^{(j_1)}$. The optimum values of $I$ and $J_2$ can be found in this case. Moreover,

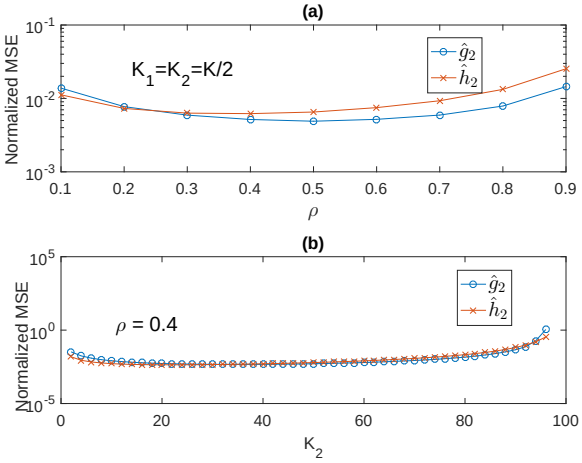


Fig. 3. Normalized MSE of $\hat{g}_2$ and $\hat{h}_2$ vs. $\rho$ and $K_2$ for $\gamma_g = \gamma_h = 10\ dB$ with fixed channel realization in Scheme 2.

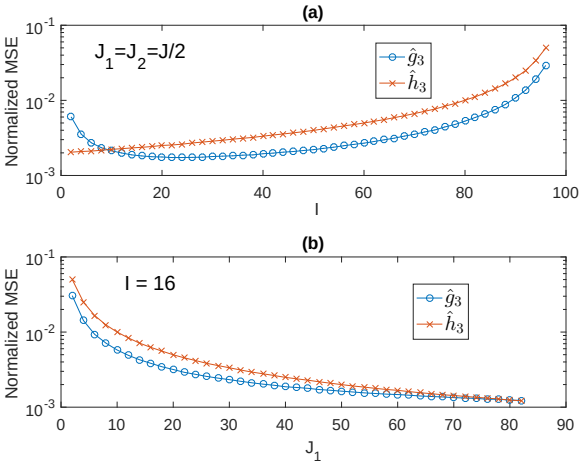


Fig. 4. Normalized MSE of $\hat{g}_3$ and $\hat{h}_3$ vs. $I$ and $J_1$ for $\gamma_g = \gamma_h = 10\ dB$ with fixed channel realization in Scheme 3.

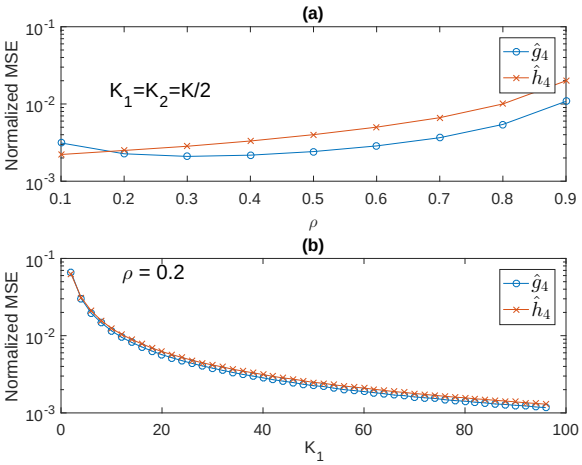


Fig. 5. Normalized MSE of $\hat{g}_4$ and $\hat{h}_4$ vs. $\rho$ and $K_1$ for $\gamma_g = \gamma_h = 10\ dB$ with fixed channel realization in Scheme 4 .

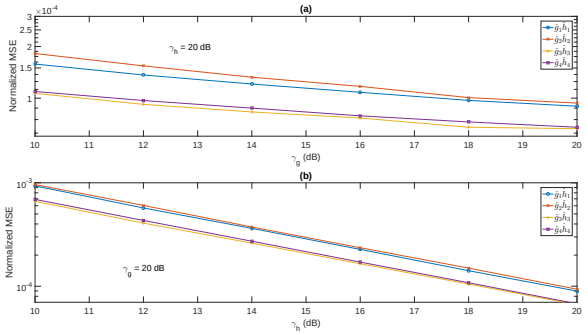


Fig. 6. Minimum normalized MSE of $\hat{g}\hat{h}$ vs. $\gamma_g$ and $\gamma_h$ for different schemes with fixed channel realization.

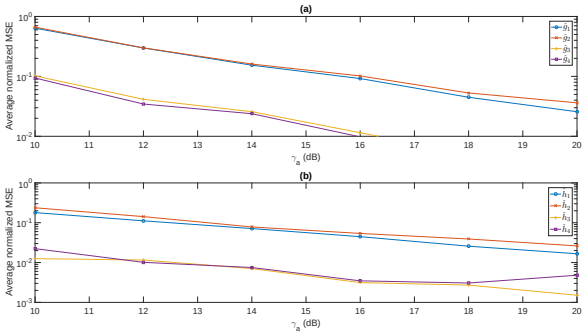


Fig. 7. The average normalized MSEs of $\hat{g}$ and $\hat{h}$ vs. $\gamma_a$ for different schemes over different channel realizations.

there is a wide range of choices for $I$ and $J_2$ that give close-to-optimum performances. This provides flexibility in system design. Secondly, the performance of $\hat{g}_1$ is close to that of $\hat{h}_1$, especially near the optimum values of $I$ and $J_2$.

Fig. 3 shows the normalized MSE of $\hat{g}_2$ and $\hat{h}_2$ versus $\rho$ and $K_2$, for $\hat{g}_2 = \hat{h}_2 = 10\ dB$ in Scheme 2. In Fig. 3.(a), the value of $\rho$ is varied from 0.1 to 0.9 with a step size of 0.1, when $K_1 = K_2 = \frac{K}{2}$. In Fig. 3.(b), the value of $K_2$ is examined from 4 to 96 with a step size of 4, when $\rho = 0.4$. In this figure, the optimum value of $\rho$ exists. For $\rho$, when it is large, more energy is harvested for relay transmission but the signal component in the samples will be weaker, leading to more estimation errors. Thus, a balanced choice of $\rho$ needs to be made and it plays a similar role to $\frac{I}{K}$ in Scheme 1. Also, compared with Fig. 2, there is a wider range of choices for $K_2$ that can achieve close-to-optimum performance.

Fig. 4 shows the normalized MSE of $\hat{g}_3$ and $\hat{h}_3$ versus $I$ and $J_1$ in Scheme 3. In Fig. 4.(a), the value of $I$ is varied from 4 to 96 with a step size of 4, when $J_1 = J_2 = \frac{J}{2}$. Also, in Fig. 4.(b), the value of $J_1$ is examined from 2 to $J-2$ with a step size of 2, while $I = 16$. From this figure, the normalized MSE monotonically increases with $I$ and decreases with $J_1$ in most cases. Also, $\hat{g}_3$ has a smaller normalized MSE than $\hat{h}_3$ in most cases. Fig. 5 shows the normalized MSE versus $\rho$ and $K_1$ in Scheme 4. As can be seen from Fig. 5, the normalized MSE increases with $\rho$ and decreases with $K_1$.

Fig. 6 compares the estimators in terms of their minimum normalized MSEs of $\hat{g}\hat{h}$ in fixed channel realization achieved

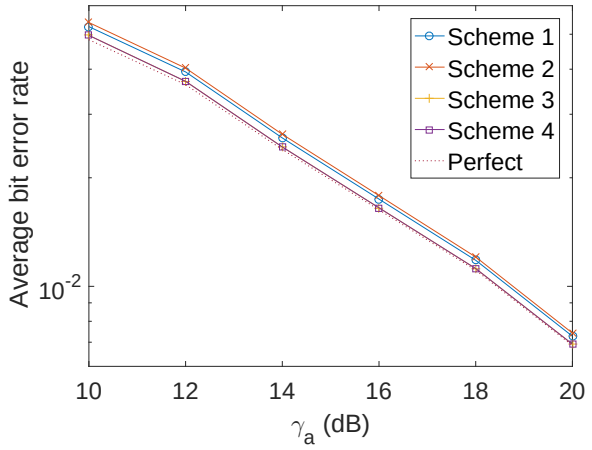


Fig. 8. The average BER vs. $\gamma_a$ for different schemes over different channel realizations.

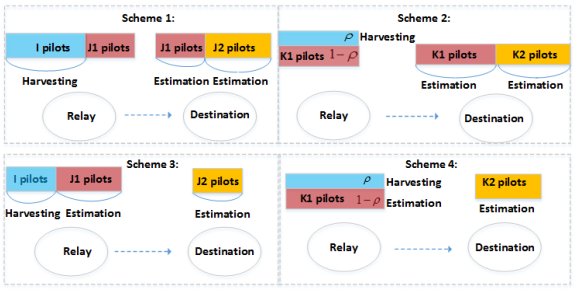


Fig. 9. Diagrams of different energy harvesting channel estimation schemes.

by performing exhaustive searches over the relevant parameters. One sees that Scheme 3 and Scheme 4 outperform Scheme 1 and Scheme 2 in this case.

Figs. 7 and 8 show the average normalized MSE and average BER vs. $\gamma_a$ over different channel realizations, respectively. In these figures, $I = 40$ and $J_2 = 20$ for Scheme 1, $\rho = 0.5$ and $K_2 = 20$ for Scheme 2, $I = 16$ and $J_1 = 64$ for Scheme 3, $\rho = 0.2$ and $K_1 = 80$ for Scheme 4. These values may not be optimum but are fixed to have reasonable calculation time. One sees that the average normalized MSE and average BER always decrease when $\gamma_a$ increases. For the average normalized MSE, $\hat{h}$ is better than $\hat{g}$, and Scheme 1 and Scheme 2 are worse than Scheme 3 and Scheme 4. For the average BER, all the estimators have performances very close to the perfect case when there is no channel estimation error in the demodulation. Scheme 3 and Scheme 4 have slightly smaller average BER than Scheme 1 and Scheme 2, which agrees with the observations in Fig. 7.(a) for different channel realizations.

Fig. 9 compares the different characteristics of the proposed schemes. In summary, Scheme 1 uses TS and only performs channel estimation at the destination, Scheme 2 uses PS and only performs channel estimation at the destination, Scheme 3 uses TS and performs channel estimation at both the relay and the destination, while Scheme 4 uses PS and performs channel estimation at both the relay and the destination. Among the proposed schemes, Scheme 1 and Scheme 2 have minimum energy and complexity requirements on the relay, as the energy is supplied by the source and the relay does not perform channel estimation either. Thus, they are suitable for machine-to-machine communications [24], where the relay is a peer node sensitive to both energy and complexity requirements. On the other hand, Scheme 3 and Scheme 4 are suitable for infrastructure-based relaying, where the relay is a fixed node and is not sensitive to complexity [25]. Thus, the motivation of providing all these schemes are two-fold. From the performance's perspective, Scheme 3 and Scheme 4 are better than Scheme 1 and Scheme 2. For example, in Fig. 6.(a), Scheme 1 and Scheme 2 have a normalized MSE of about $2\times10^{-4}$ at $\gamma_g = 10\ dB$, while Scheme 3 and Scheme 4 have a normalized MSE of about $1\times10^{-4}$, only half of that for Scheme 1 and Scheme 2. In Fig. 7.(a), Scheme 3 and Scheme 4 have an average normalized MSE of 0.1 at $\gamma_a = 10\ dB$, much smaller than the average normalized MSE of 0.6 for Scheme 1 and Scheme 2. These performance differences are significant. Even for the BER performance, in Fig. 8 at $BER = 10^{-2}$, Scheme 3 and Scheme 4 have a considerable gain of around 0.2 dB over Scheme 1 and Scheme 2. From the complexity's perspective, Scheme 1 and Scheme 2 are simpler than Scheme 3 and Scheme 4, as they do not perform channel estimation at the relay and they do not need to feed the channel estimate to the destination either. These differences in performance and complexity allow the estimators to be used in different applications that have different requirements, such as machine-to-machine communications and infrastructure-based relaying, which motivate us to consider all of them.

The theoretical values for the optimum $I$, $J_1$, $J_2$, $K_1$, $K_2$ and $\rho$ could be calculated by deriving the analytical expressions of the performance measures and optimizing these performance measures. However, such calculation is very difficult, if not impossible. Thus, we rely on an exhaustive search to find these values. Nevertheless, from Figs. 2 - 5, the performance is not very sensitive to the choices of these parameters and there is often a wide range of choices that provide close-to-optimum performance. This does not mean that the performance is not sensitive to the overall sample size $K$.

## V. Conclusion

New pilot-based MB estimators for AF relaying have been proposed that use energy harvesting. Numerical results have been presented to show their performances. In terms of complexity, Scheme 1 and Scheme 2 are the simplest, as they require neither channel estimation at the relay nor channel estimate feedback to the destination while Scheme 3 and Scheme 4 do have these extra requirements. In terms of MSE performance, Scheme 3 and Scheme 4 have the smallest MSE. In terms of BER performance, all schemes are close to the perfect case, while Scheme 3 and Scheme 4 are slightly better than Scheme 1 and Scheme 2. These conclusions are made from Figs. 6 - 8 based on the specific settings given in the first paragraph of the previous section. However, they may not be general for all scenarios. Note that the proposed estimators use pilots only. This is similar to some previous work in [9] - [14].

Thus, no data symbols are available for energy harvesting in the estimation. One could extend this scheme to blind or semi-blind estimation, enabling energy to be harvested from data symbols. One could also consider optimal power allocation with respect to the ratio of pilots to data symbols in a frame with fixed length [26], [27]. Furthermore, one could assume a direct link between source and destination and compare the performance with indirect relaying. Finally, when the relay sends pilots to the destination, it can also harvest energy from its own transmitted pilots. However, this requires a more complicated full-duplex radio that can perform transmission and reception at the same time [28], [29]. This work only considers half-duplex radio that is widely used in wireless systems, and in this case the relay cannot harvest energy from its own transmitted pilots.

## ACKNOWLEDGMENT

The authors would like to thank Dr. Richard Staunton for kindly proofreading the manuscript.

## REFERENCES

[1] A.A. Nasir, X. Zhou, S. Durrani, R.A. Kennedy, "Relaying protocols for wireless energy harvesting and information processing," *IEEE Trans. Wireless Commun.*, vol. 12, pp. 3622 -3636, July 2013.

[2] Z. Ding, S.M. Perlaza, I. Esnaola, H.V. Poor, "Power allocation strategies in energy harvesting wireless cooperative networks," *IEEE Trans. Wireless Commun.*, vol. 13, pp. 846 - 860, Feb. 2014.

[3] Y. Chen, "Energy harvesting AF relaying in the presence of interference and Nakagami-$m$ fading," *IEEE Trans. on Wireless Commun.*, to appear.

[4] B. Carvalho *et al*, "Wireless power transmission: R&D activities within Europe," *IEEE Trans. Microwave Theo. and Tech.*, vol. 62, pp. 1031 - 1045, Apr. 2014.

[5] F. Azmat, Y. Chen, N. Stocks, "Predictive modelling of RF energy for wireless powered communications," *IEEE Commun. Lett.*, vol. 20, pp. 173 - 176, Jan. 2016.

[6] S. Sudevalayam, and P. Kulkarni, "Energy harvesting sensor nodes: survey and implications," *IEEE Communications Surveys and Tutorials*, vol. 13, pp. 443 - 461, Sept. 2011.

[7] L. R.Varshney, "Transporting information and energy simultaneously, in *Proc. IEEE Int. Symp. Inf. Theory*, pp. 16121616, June 2008.

[8] X. Zhou, R. Zhang, C.K. Ho, "Wireless information and power transfer: architecture design and rate-energy tradeoff," *IEEE Trans. Commun.*, vol. 61, pp. 4754 - 4767, November 2013.

[9] C.S. Patel and G.L. Stuber, "Channel estimation for amplify and forward relay based cooperation diversity systems," *IEEE Trans. Wireless Commun.*, vol. 6, pp. 2348 - 2356, June 2007.

[10] F. Gao, T. Cui, A. Nallanathan, "On channel estimation and optimal training design for amplify and forward relay networks," *IEEE Trans. Wireless Commun.*, vol. 7, pp. 1907 - 1916, May 2008.

[11] A.S. Behbahani and A. Eltawil, "On channel estimation and capacity for amplify and forward relay networks," *Proc. IEEE Globecom 2008*, pp. 1 - 5, New Orleans, USA, 2008.

[12] O. Amin, B. Gedik, M. Uysal, "Channel estimation for amplify-and-forward relaying: cascaded against disintegrated estimators," *IET Commun.*, vol. 4, pp. 1207 - 1216, 2010.

[13] F.A. Khan, Y. Chen, M.-S. Alouini, "Novel receivers for AF relaying with distributed STBC using cascaded and disintegrated channel estimation," *IEEE Trans. Wireless Commun.*, vol. 11, pp. 1370 - 1379, Apr. 2012.

[14] H. Yomo and E. de Carvalho, "A CSI estimation method for wireless relay networks," *IEEE Commun. Lett.*, vol. 11, pp. 480 - 482, June 2007.

[15] M. Peng, Y. Liu, D. Wei, W. Wang, H.-H. Chen, "Hierarchical cooperative relay based heterogeneous networks," *IEEE Wireless Commun.*, vol. 18, pp. 48 - 56, June 2011.

[16] B. Zhou, H. Hu, S.-Q. Huang, H.-H. Chen, "Intracluster device-to-device relay algorithm with optimal resource allocation," *IEEE Trans. Veh. Technol.*, vol. 62, pp. 2315 - 2326, June 2013.

[17] M.O. Hasna and M.-S. Alouini, "A performance study of dual-hop transmissions with fixed gain relays," *IEEE Trans. on Wireless Commun.*, vol. 3, pp. 1963-1968, Nov. 2004.

[18] M. Di Renzo, F. Graziosi and F. Santucci, "A comprehensive framework for performance analysis of dual-hop cooperative wireless systems with fixed-gain relays over generalized fading channels," *IEEE Trans. on Wireless Commun.*, vol. 8, pp. 5060-5074, Oct. 2009.

[19] T. Le, K. Mayaram, T. Fiez, "Efficient far-field radio frequency energy harvesting for passively powered sensor networks," *IEEE J. Solid-State Circuits*, vol. 43, pp. 1287 - 1302, May 2008.

[20] J. Yi, W.-H. Ki, C.-Y. Tsui, "Analysis and design strategy of UHF micro-power CMOS rectifiers for micro-sensor and RFID applications," *IEEE Trans. Circuits and Systems I*, vol. 54, pp. 153 - 166, Jan. 2007.

[21] S. Kay, *Fundamentals of Statistical Signal Processing: Estimation Theory*, Prentice Hall: London, 1993.

[22] I.S. Gradshteyn and I.M Ryzhik, *Table of Integrals, Series and Products*, 7th Ed. Academic Press: London, UK. 2007.

[23] G.L. Stuber, *Principles of Mobile Communication*, 2nd Ed. Kluwer Academic: London, 2001.

[24] S.-C. Lin, K.-C. Chen, "Cognitive and opportunistic relay for QoS guarantees in machine-to-machine communications," *IEEE Trans. Mobile Computing*, vol. 15, pp. 599 - 609, Mar. 2016.

[25] A. Adinoyi, H. Yanikomeroglu, "Cooperative relaying in multi-antenna fixed relay networks," *IEEE Trans. Wireless Commun.*, vol. 6, pp. 533 - 544, Feb. 2007.

[26] Y. Chen and N.C. Beaulieu, "Optimum pilot symbol assisted modulation," *IEEE Trans. on Commun.*, vol. 55, pp. 1536-1546, Aug. 2007.

[27] K. Wang, Y. Chen, M.-S. Alouini, F. Xu, "BER and optimal power allocation for amplify-and-forward relaying using pilot-aided maximum likelihood estimation," *IEEE Trans. Commun.*, vol. 62, pp. 3462 - 3475, Oct. 2014.

[28] C. Zhong, H.A. Suraweera, G. Zheng, I. Krikidis, Z. Zhang, "Wireless information and power transfer with full deplex relaying," *IEEE Trans. Wireless Commun.*, vol. 62, pp. 3447 - 3461, Oct. 2014.

[29] S. Hu, Z. Ding, Q. Ni, "Beamforming optimisation in energy harvesting cooperative full-duplex networks with self-energy recycling protocol," *IET Commmun.*, vol. 10, pp. 848 - 853, 2016.